2014 Tenth International Conference on Signal-Image Technology & Internet-Based Systems

# Accurate Detection of Non-Iris Occlusions

Michal Haindl* Mikuláš Krupička *†
*Institute of Information Theory and Automation of the ASCR**
*182 08 Prague, Czech Republic*
*Email: {haindl,krupimik}@utia.cas.cz*
*Faculty of Information Technology†*
*Czech Technical University*
*160 00 Prague, Czech Republic*

***Abstract*—Accurate detection of iris eyelids and reflections is the prerequisite for the accurate iris recognition, both in near-infrared or visible spectrum measurements. Undected iris occlusions otherwise dramatically decrease the iris recognition rate. This paper presents a fast multispectral iris occlusions detection method based on the underlying multispectral spatial probabilistic iris textural model and adaptive thresholding. The model adaptively learns its parameters on the iris texture part and subsequently checks for iris reflections, eyelashes, and eyelids using the recursive prediction analysis. Our method obtains better accuracy with respect to the previously performed Noisy Iris Challenge Evaluation contest. It ranked first from the 97+2 alternative methods on this large colour iris database.**

***Keywords*-iris occlusions; detection; textural model;**

## I. Introduction

Biometrics based human identification systems have ever growing importance in recent trends towards more secure modern information society. Diverse biometric data can be exploited for numerous practical applications, such as bank access, airport entry points, or criminal evidence gathering but also for smart homes, cars control, or handicapped help systems. It can be human voice, fingerprint, eye, face, gait, veins, handwriting and many more. Various biometric data differ in ways how to acquire them, their durability, reliability, safety, and necessary technology for their acquisition and evaluation.

In this work we focus on preprocessing part of the iris recognition - iris occlusion detection. The possibility for the eye-based human identification was originally suggested by [1] and later estimated that the probability of two similar iris is 1 in $10^{72}$ [2]. For recent surveys of the iris recognition related problems and results see [3], [4].

The iris identification is complex task composed from several steps (see the processing schema on Fig.1 with iris occlusion detection elaborated part) that have to be solved. The whole process starts with image acquisition which hardly produces ideal noise-free, focused, and homogeneously illuminated images, thus the corresponding preprocessing steps for data normalization, denoising, or geometric corrections are inevitable before the iris segmentation can be performed. The iris segmentation results are typically coordinates of two circles, inner and outer border of iris. Additionally, a normalization step has been introduced to simplify the subsequent processing steps.

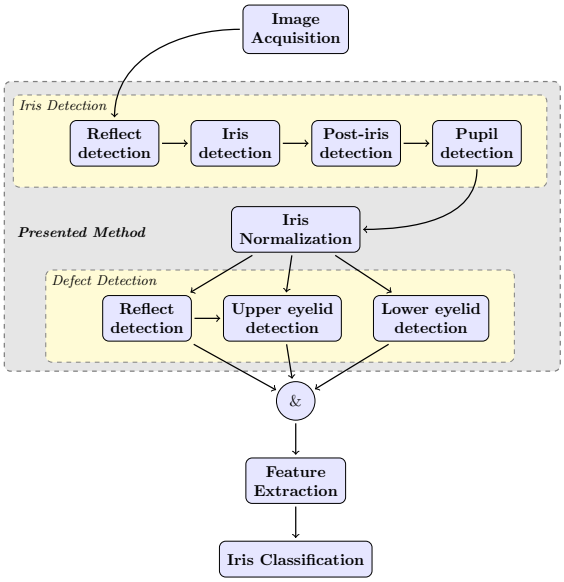


Figure 1. Iris recognition processing pipeline .

Normalization is usually done transforming the iris into a fixed size rectangle. The selected features are then computed from the normalized rectangle and used in a classifier to recognize a corresponding human.

Unconstrained iris measurements contain numerous occlusion defects such as eyelid, eyelash, and reflections which have to be detected in the preprocessing step of any iris recognition algorithm. Undetected occlusions would otherwise confuse the recognition method and impair its recognition rate. While the unconstrained visible wavelength iris image acquisition is cheap and widely available it requires more demanding iris processing methods to achieve comparable recognition rate with the rigid optimal acquisition conditions.

### A. Iris Occlusions Detection

Unconstrained iris measurements inevitably introduce various sensing imperfections, such as reflections, upper / lower eyelids or eyelashes occlusions, or eyelid shadows. Such undetected occlusions significantly degrade iris classifiers performance. Thus it is necessary to remove such areas from the iris texture prior to the classification process

978-1-4799-7978-3/14 $31.00 © 2014 IEEE
DOI 10.1109/SITIS.2014.48

what constitutes on of the most challenging problem in the iris recognition research [2]. Some detection methods are specialized to single imperfection category only, while others [5]–[16] can detect several types of imperfections.

Methods focused only on reflections are based on (adaptive) thresholding (eg. [17]). Eyelid detectors are mostly based on edge detection followed with polynomial fitting (eg. [18], [19]). Chen *et al.* [20] or He *et al.* [21] proposed methods of eyelash detection based on simple thresholding, One of the first general imperfection detection methods was presented by Proenca [11]. His method is based on training classifier on manually detected irises and the eye representation is based on textural GLCM [22] features and the detector uses a neural network classifier.

The conventional approach for defect detection [23] is to compute a texture features in a local sub-window and to compare them with the reference values representing a perfect pattern. The method [24] preprocesses a gray level textile texture with histogram modification and median filtering. The image is subsequently thresholded using the adaptive filter and finally smoothed with another median filter run. Another approach for detection of gray level textured defects using linear FIR filters with optimized energy separation was proposed in [25]. Similarly the defect detection [26] is based on a set of optimized filters applied to wavelet sub-bands and tuned for a defect type. Method [27] uses translation invariant 2D RI-Spline wavelets for textile surface inspection. The gray level texture is removed using the wavelet shrinkage approach and defects are subsequently detected by simple thresholding. The method [16] is based on textural Gabor features and the Gaussian mixture model to model the underlying probability distributions of both defect and iris regions. Contrary to above approaches the presented method uses the visible wavelength multispectral information.

Recent state-of-the-art non-iris occlusions detectors were mostly competing in the 2008 NICE.I (Noisy Iris Challenge Evaluation) focusing especially on detection accuracy. Nearly hundred various methods from 22 countries were submitted to this challenge and the best-ranked algorithms were published in [28]. The presented method uses these best-ranked algorithms for comparison. Anyhow, contrary to our method none of these NICE methods use true multispectral information. The source images (which are in RGB colour space) are typically either converted to grey-scale before any analytical steps or only one spectrum channel is used.

The 2008 NICE.I best method by Tan et al. [13] uses clustering based on coarse iris localization after previously removed reflections. In the subsequent step it refines the iris and pupil location using the Daugman's integrodifferential operator. Finally, the prediction and curvature models are learned to deal with eye occlusions such as eyelids and eyelashes.

The second best method by Sankowski et al. [12] consists of three steps - threshold based reflections detection, iris boundaries detection based on the modified Daugman's integro-differential operator, and eyelids detection

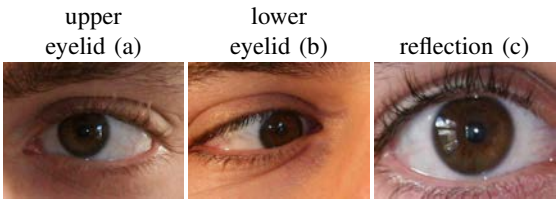


Figure 2. Iris region occlusions containing all three (a,b,c) occlusion types.

based on parametric modelling. The iris outer boundary is searched in greyscale image based on YIQ model while the inner is searched in red channel. Lastly, the lower eyelid boundary is modeled as circular arc and upper eyelid boundary is modeled as straight edge.

The third method by Pedro Almeida [6] is based on an expert system with set of decision rules which mainly present novel iris boundary detection and upper and lower eyelid arc fitting. These rules were based on concepts identified by human (the teaching system) as the criteria identified by him when performing the same task.

The fourth NICE.I 2008 contest method is from Li et al. [9]. It starts with eye detection and then localize iris and pupil boundaries using K-Means algorithm combined with the modified Hough transformation. In the case of detected wrong localization they try to localize iris using the second algorithm based on skin information. Then lower eyelid is detected by fittin parabola and upper eyelid is detected by running parabolic integrodifferential operator combined with RANSAC-like technique.

Jeong et al. [7] presented another algorithm to detect eye occlusions. The inner and outer boundaries of iris region are detected using circular edge detector. In case of bad detection (based on the existence of corneal specular reflection) they run additional Adaboost classificator to roughly localize the eye position. For eyelids they use parabolic Hough transform and for reflections color segmentation. Lastly, they proposed a classification model to detect closed eye.

Chen et al. [5] proposed an algorithm composed from five steps. They firstly locate the rough position of eye using the extracted sclera area. Then detect the outer iris boundary with circular Hough transform followed by detection of upper and lower eyelids by detecting linear edge using Hough transform. Lastly they detect the pupil area by threshold detection. Several other NICE.I algorithms (Markovian texture model [15], Zernike feature based classification [14], are used to compare the presented method.

## II. Iris Localization

The iris occlusions (Fig.2) detection starts with searching for reflections (Fig.3-left) in the blue spectral channel where they are the most visible (according to our extensive experiments) using an adaptive threshold. The binarization threshold is obtained using the cross-correlation between pixel-centered windows and the Gaussian window. The

Figure 3. Iris detected reflections (middle) and their corrections.

resulting binary mask is firstly slightly dilated (Fig.3-middle) to ensure full coverage of reflections and than the detected reflective regions are corrected (Fig.3-right) using the inpainting algorithm preseted in [29]. The corrected image is subsequently used to detect iris location in the image. The eye area is found using the modified integro-differential Daugman operator [30]

$$\max_{\rho,\tilde{r}_1,\tilde{r}_2} \left| G_\sigma(\rho) * \frac{\partial}{\partial \rho} \oint_{\rho,\tilde{r}_1,\tilde{r}_2} \frac{Y_{r,B}}{2\pi\rho} ds d\rho \right| \quad , \qquad (1)$$

where $r = \{r_1, r_2\}, s = \{s_1, s_2\}$ are multiindices with the row and column indices, $\tilde{r}$ the radius centre, $\rho$ is the radius, $Y_{r,B}$ is the blue component of the r-th eye pixel, and $G_\sigma(\rho)$ denotes a Gaussian filter of scale $\sigma$. However the circle integral is not taken for full circle but only for degrees from $0°$ to $45°$ and from $135°$ to $360°$. This is to better deal with possible upper eyelid occlusions in image (which would otherwise obviously obstruct the correct localization of iris region). Fig.4-left illustrates local maxima (white dots) in the accumulator of this operator. Fig.4-right images show the localized iris regions where the outer circles correspond to global maxima of this accumulator.

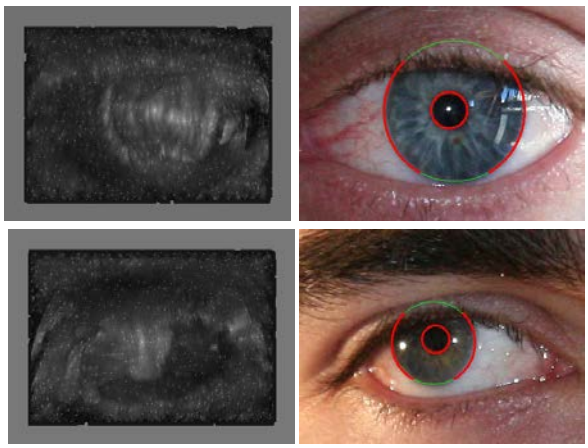

Figure 4. The accumulator of the integro-differential Daugman operator (1) in the blue spectral channel (left) and the resulting iris localization.

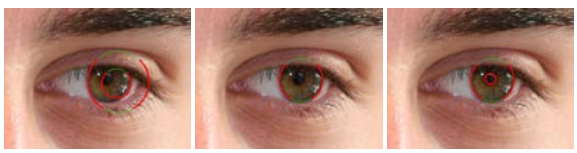

Figure 5. Imprecisely detected iris region (left), its correction (middle) and the corrected pupil (right).

The next step is the pupil detection in the red spectral channel to separate iris region due to its best separability spectrum. The inner circle representing pupil border is found in a similar way as the iris location described above but in its respective smaller area. The pupil is detected using the original (unmodified) Daugman operator inside the iris region. Detected iris region is then verified by checking the candidate pupil region mean with comparison of the closest left and right neighbourhood iris regions. This is to deal with possible mislocalization of iris border as can be seen in Fig.5.

## III. Iris Occlusions and Reflection Detection

Once we locate the iris region, this region is then normalized to rectangular shape and we subsequently search for each of the selected occlusions (as can be seen in Fig.1). Possible occlusions are searched in the red spectral channel and reflections in the blue spectral channel, respectively.

### A. Upper Eyelid

The normalization step iris transformation concentrates the lower eyelid near the image center but the upper eyelid is separated at the left and right margins of the image. Hence, the image is first vertically swapped to place the potential upper eyelid (Fig.2-left) to the center. Then the rays are drawn from the top center point in the angular range $0°$ to $180°$ with $5°$ spacing. The pixels on these rays are sampled to lines, they are convolved with the Gaussian kernel, and the maximum is located on each of them. Finally, the third order fitted polynomial denotes the upper eyelid occlusion region border.

### B. Lower Eyelid

Most iris images are not obstructed with the lower eyelid. The occasional lower eyelid occlusions (Fig.2-middle) are detected using mean and standard deviation estimates $\mu_{le}$ and $\sigma_{le}$ of the top center region. Rows are in the range of $r_1 \in \langle 0; \frac{N}{2} \rangle$ and columns $r_2 \in \langle \frac{M}{4}; \frac{3M}{4} \rangle$, where $N$ $(M)$ is number of rows (columns) in the normalized iris image. If the standard deviation is larger than $25\%$ of $\mu_{le}$, i.e.,

$$\sigma_{le} > \frac{\mu_{le}}{4}$$

then the lower eyelid is detected by simple thresholding with the threshold $\tau = \mu + \frac{\sigma_{le}}{2}$. The topmost central region is detected as the lower eyelid in the resulting binarized image.

### C. Iris Reflections

The precise localization of reflections (Fig.2-right) is based on fusion of similar (without dilatation) adaptive thresholding as in section II and detection based on the multispectral Markovian iris texture model.

*1) Iris Spectral Texture Model:* We assume that the multispectral iris texture can be represented by an adaptive 3D causal simultaneous auto-regressive model [31]:

$$X_r = \sum_{s \in I_r^c} A_s X_{r-s} + \epsilon_r \ , \tag{2}$$

where $\epsilon_r$ is a white Gaussian noise vector with zero mean, and a constant but unknown covariance matrix $\Sigma$. The noise vector is uncorrelated with data from a causal neighbourhood $I_r^c$, and $r = \{r_1, r_2\}, s = \{s_1, s_2\}$ are multiindices with the row and column indices, respectively.

$$A_{s_1,s_2} = \begin{pmatrix} a_{1,1}^{s_1,s_2}, \ldots, a_{1,d}^{s_1,s_2} \\ \vdots, \ddots, \vdots \\ a_{d,1}^{s_1,s_2}, \ldots, a_{d,d}^{s_1,s_2} \end{pmatrix} \tag{3}$$

are $d \times d$ parameter matrices where $d$ is the number of spectral bands. $r, r-1, \ldots$ is a chosen direction of movement on the image lattice (e.g. scanning lines rightward and top to down). All parameters in this model can be analytically estimated using numerically robust recursive statistics hence it is exceptionally well suited for possibly real-time recursive iris texture occlusion detectors.

The model adaptivity is introduced using the exponential forgetting factor technique in the parameter learning part of the algorithm. The causality of the model, which is artificial for visual iris data, does not create any problem for our analytical application and furthermore, it is fully compensated by the introduced adaptivity of the model. The model can be alternatively written in the matrix form

$$X_r = \gamma Z_r + \epsilon_r \ , \tag{4}$$

where

$$\begin{aligned} \gamma &= [\, A_1, \ldots, A_\eta \,] \ , \\ \eta &= cardinality(I_r^c) \ , \end{aligned}$$

is a $d \times d\eta$ parameter matrix and $Z_r$ is a corresponding vector of $X_{r-s}$. To evaluate the conditional mean values $E\{X_r \,|\, X^{(r-1)}\}$ , where $X^{(r-1)}$ is the past process history, the one-step-ahead prediction posterior density $p(X_r \,|\, X^{(r-1)})$ is needed. If we assume the normal-gamma parameter prior for parameters in (2) this posterior density has the form of Student's probability density with $\beta(r) - d\eta + 2$ degrees of freedom. The predictor in the form of conditional mean value (9) uses the following notation (5)-(8):

$$\begin{aligned} \beta(r) &= \beta(0) + r - 1 \ , & (5) \\ \hat{\gamma}_{r-1}^T &= V_{zz(r-1)}^{-1} V_{zx(r-1)} \ , & (6) \\ V_{r-1} &= \begin{pmatrix} \tilde{V}_{xx(r-1)} & \tilde{V}_{zx(r-1)}^T \\ \tilde{V}_{zx(r-1)} & \tilde{V}_{zz(r-1)} \end{pmatrix} + I \ , & (7) \\ \tilde{V}_{uw(r-1)} &= \sum_{k=1}^{r-1} U_k W_k^T \ , & (8) \end{aligned}$$

where $\beta(0) > 1$ and $U, W$ denote either $X$ or $Z$ vector, respectively. If $\beta(r-1) > \eta$ then the conditional mean value is

$$E\{X_r | X^{(r-1)}\} = \hat{\gamma}_{r-1} Z_r \tag{9}$$

and it can be efficiently computed using the following recursion [31]:

$$\hat{\gamma}_r^T = \hat{\gamma}_{r-1}^T + \frac{V_{z(r-1)}^{-1} Z_r (X_r - \hat{\gamma}_{r-1} Z_r)^T}{1 + Z_r^T V_{zz(r-1)}^{-1} Z_r} \ . \tag{10}$$

The selection of an appropriate model support $(I_r^c)$ is important to obtain good iris representation. If the contextual neighbourhood is too small it can not capture all details of the random field iris texture model. Inclusion of the unnecessary neighbours on the other hand adds to the computational burden and can potentially degrade the performance of the model as an additional source of noise. The optimal Bayesian decision rule for minimizing the average probability of decision error chooses the maximum posterior probability model, i.e., a model $M_i$ corresponding to

$$\max_j \{p(M_j | X^{(r-1)})\}$$

can be easily found analytically [31].

*2) Reflection Detection:* Single multispectral pixels are classified as belonging to the defective (non-iris) area based on their corresponding prediction errors. If the prediction error is larger than the adaptive threshold:

$$\begin{aligned} &|\tilde{E}\{X_r \,|\, X^{(r-1)}\} - X_r| > \\ &\frac{\alpha}{l} \sum_{i=1}^{l} \left| \tilde{E}\{X_{r-i} \,|\, X^{(r-i-1)}\} - X_{r-i} \right| \ , \end{aligned} \tag{11}$$

then the pixel $r$ is classified as a detected occlusion pixel. The parameter $l$ in (12) is a process history length of the adaptive threshold and the constant $\alpha = 2.7$ was found experimentally and used for all three tested databases.

The one-step-ahead predictor

$$\tilde{E}\{X_r \,|\, X^{(r-1)}\} = \hat{\gamma}_s \, Z_r \tag{12}$$

differs from the corresponding predictor (9) in using parameters $\hat{\gamma}_s$ which were learned only in the flawless texture area $(s < r)$. The small learning flawless texture cutout is found automatically inside reflection-less iris area. The whole algorithm is extremely fast because the adaptive threshold is updated recursively:

$$|\epsilon_{r+1}| > \frac{\alpha}{l} \left[ \sum_{i=0}^{l-1} |\epsilon_{r-i}| \right] \ , \tag{13}$$

where $\epsilon_r$ is the prediction error

$$\epsilon_r = \tilde{E}\{X_r \,|\, X^{(r-1)}\} - X_r \ ,$$

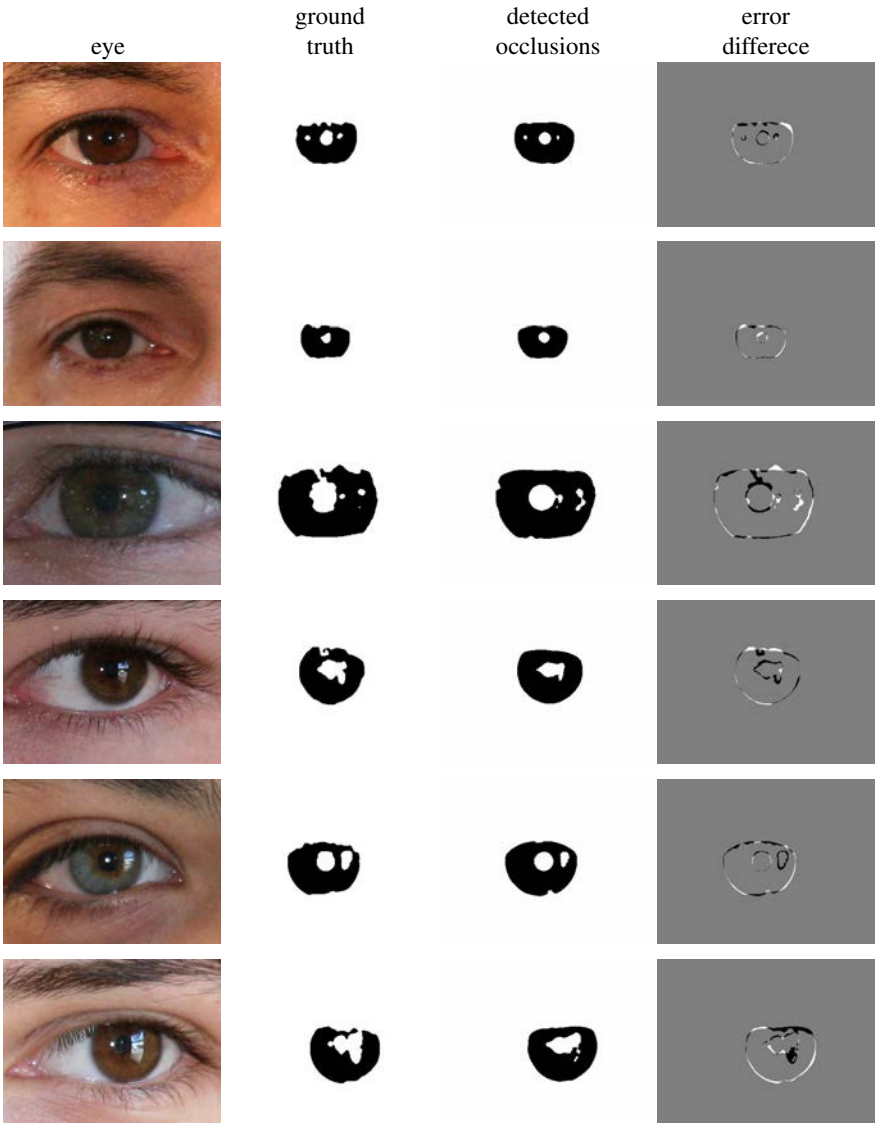


Figure 6. Eye images, ground truth, detected occlusions masks, and their comparison with the ground truth.

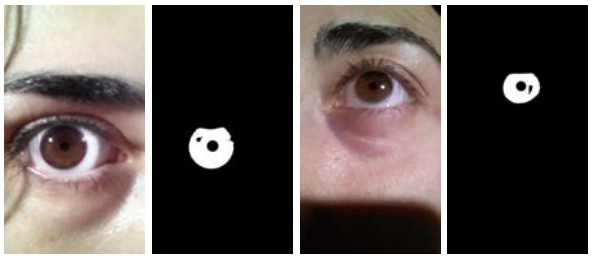

Figure 7. Detected iris region occlusions on the MICHE database [32].

and $\hat{\gamma}_s$ is the parametric matrix which is not changing. Hence the algorithm can be easily applied in real time iris occlusion detection.

## IV. Experimental Results

The presented method was tested on the eye UBIRIS.v2 database [33] and compared with the best results achieved during the Noisy Iris Challenge Evaluation contest [28] using exactly the same conditions which held for the contest participants. These databases provide eye images with or without different occlusion types (Fig.2), and thus are an useful resource for the evaluation iris recognition methods.

The UBIRIS.v2 database [34] contains 11102 images collected from 261 persons. The RGB $400 \times 300$, 24 bit images were captured with the Canon EOS 5D camera and saved in the TIFF format. The presented method was compared with the top eight results (from 97 participants) [5]–[10], [12], [13] from the Noisy Iris Challenge Evaluation Contest (NICE.I) [28] and results using the same NICE.I data presented in the paper [14]. The contest was run on

the UBIRIS.v2 database which contains highly noisy eye images. The participants had 500 training images and a disjoint test set of 500 images was used to measure the pixel-by-pixel agreement between the binary maps made by each participant and the ground-truth data, manually built by the NICE.I organizers.

Fig.6 indicates several types of defective iris textures. This example illustrates correct detection and localization of the most frequented iris occlusion by the presented method.

The presented method ranked first (Tab.I) according to the contest criterion $E_1$ [9]. Some methods evaluated also the average between false-positives and false-negatives criterion $E_2$ [9]. No. par. is the number of parameters of the listed methods. The Noisy Iris Challenge Evaluation Contest winning algorithm [13] has slightly worse performace than the presented method but it is very complex, time consuming and suffers with numerous experimentally set control parameters. Similarly the third ranked method [12] based on the reflections localization, reflections filling in, iris boundaries localization and eyelids boundaries localization steps, relies on several experimentally found parameters.

Table I
IRIS OCCLUSION DETECTION NOISY IRIS CHALLENGE EVALUATION CONTEST [28] TOP EIGHT RESULTS ON THE CONTEST UBIRIS V2 DATABASE COMPARED WITH THE PRESENTED METHOD AND [14], [15].

| Rank | Method | No. par. | Error $\mathbf{E}_1$ | $E_2$ |
|---|---|---|---|---|
| 1 | **presented method** | 7 | **0.0124** | 0.042 |
| 2 | Tan et al. [13] | 9 | 0.0131 | - |
| 3 | Sankowski et al. [12] | 6 | 0.0162 | 0.060 |
| 4 | Haindl & Krupička [15] | 2 | 0.0168 | 0.061 |
| 5 | Almeida [6] | 5 | 0.0180 | - |
| 6 | Tan & Kumar [14] | x | 0.0190 | - |
| 7 | Li et al. [9] | 4 | 0.0224 | 0.068 |
| 8 | Jeong et al. [7] | 3 | 0.0282 | 0.144 |
| 9 | Chen et al. [5] | 5 | 0.0297 | 0.165 |
| 10 | Scotti & Labbati [8] | 12 | 0.0301 | 0.116 |
| 11 | Luengo-Oroz et al. [10] | 7 | 0.0305 | - |

The method was also tested on the Mobile Iris Challenge Evaluation database (MICHE) [32] with promising results. There are not available ground truth data for this database thus our results can be verified only visually and no criteria value can be reported here. Fig. 7 illustrates two images from this database together with the corresponding iris detection results.

## V. CONCLUSIONS

The most published iris occlusion detection methods are monospectral, using either near-infrared or grey-scale images, while our method advantageously fully exploits both multispectral as well as the spatial information simultaneously. The method is very fast and numerically robust in comparison with the top-ranking alternative methods from the NICE.I contest. Our method ranked first when evaluated on the the Noisy Iris Challenge Evaluation Contest from the 97 competing algorithms, the Tan method, and our previously published method. Preliminary results demonstrate its promising performance also on the Mobile Iris Challenge Evaluation data. The presented method can be easily generalized for gradually changing (e.g., illumination, colour, etc.) iris texture occlusion detection by exploiting its adaptive learning capabilities.

## ACKNOWLEDGMENTS

This research was supported by grant GAČR 14-10911S.

## REFERENCES

[1] F. H. Adler, *Physiology of the eye: clinical application*. The C.V. Mosby Co., St.Louis, 1959.

[2] H. Proença and L. Alexandre, "Iris recognition: Measuring feature's quality for the feature selection in unconstrained image capture environments," in *Computational Intelligence for Homeland Security and Personal Safety, Proceedings of the 2006 IEEE International Conference on*. IEEE, 2006, pp. 35–40.

[3] K. W. Bowyer, K. Hollingsworth, and P. J. Flynn, "Image understanding for iris biometrics: A survey," *Computer vision and image understanding*, vol. 110, no. 2, pp. 281–307, 2008.

[4] M. J. Burge and K. W. Bowyer, *Handbook of iris recognition*. Springer, 2013.

[5] Y. Chen, M. Adjouadi, C. Han, J. Wang, A. Barreto, N. Rishe, and J. Andrian, "A highly accurate and computationally efficient approach for unconstrained iris segmentation," *Image and Vision Computing*, vol. 28, no. 2, pp. 261 – 269, 2010. [Online]. Available: http://www.sciencedirect.com/science/article/pii/S0262885609000833

[6] P. de Almeida, "A knowledge-based approach to the iris segmentation problem," *Image and Vision Computing*, vol. 28, no. 2, pp. 238 – 245, 2010. [Online]. Available: http://www.sciencedirect.com/science/article/pii/S0262885609001516

[7] D. S. Jeong, J. W. Hwang, B. J. Kang, K. R. Park, C. S. Won, D.-K. Park, and J. Kim, "A new iris segmentation method for non-ideal iris images," *Image and Vision Computing*, vol. 28, no. 2, pp. 254 – 260, 2010. [Online]. Available: http://www.sciencedirect.com/science/article/pii/S0262885609000638

[8] R. D. Labati and F. Scotti, "Noisy iris segmentation with boundary regularization and reflections removal," *Image and Vision Computing*, vol. 28, no. 2, pp. 270 – 277, 2010. [Online]. Available: http://www.sciencedirect.com/science/article/pii/S0262885609001073

[9] P. Li, X. Liu, L. Xiao, and Q. Song, "Robust and accurate iris segmentation in very noisy iris images," *Image and Vision Computing*, vol. 28, no. 2, pp. 246 – 253, 2010. [Online]. Available: http://www.sciencedirect.com/science/article/pii/S0262885609000754

[10] M. A. Luengo-Oroz, E. Faure, and J. Angulo, "Robust iris segmentation on uncalibrated noisy images using mathematical morphology," *Image and Vision Computing*, vol. 28, no. 2, pp. 278 – 284, 2010. [Online]. Available: http://www.sciencedirect.com/science/article/pii/S0262885609000651

[11] H. Proença and L. A. Alexandre, "A Method for the Identification of Noisy Regions in Normalized Iris Images," *18th International Conference on Pattern Recognition (ICPR'06)*, vol. 4, pp. 405–408, 2006. [Online]. Available: http://ieeexplore.ieee.org/lpdocs/epic03/wrapper.htm?arnumber=1699864

[12] W. Sankowski, K. Grabowski, M. Napieralska, M. Zubert, and A. Napieralski, "Reliable algorithm for iris segmentation in eye image," *Image and Vision Computing*, vol. 28, no. 2, pp. 231 – 237, 2010. [Online]. Available: http://www.sciencedirect.com/science/article/pii/S0262885609001103

[13] T. Tan, Z. He, and Z. Sun, "Efficient and robust segmentation of noisy iris images for non-cooperative iris recognition," *Image and Vision Computing*, vol. 28, no. 2, pp. 223 – 230, 2010. [Online]. Available: http://www.sciencedirect.com/science/article/pii/S0262885609001115

[14] C.-W. Tan and A. Kumar, "Unified framework for automated iris segmentation using distantly acquired face images," *Image Processing, IEEE Transactions on*, vol. 21, no. 9, pp. 4068–4079, 2012.

[15] M. Haindl and M. Krupička, "Non-iris occlusions detection," in *Biometrics: Theory, Applications and Systems (BTAS), 2013 IEEE Sixth International Conference on*. IEEE, September 2013, pp. 1–6.

[16] Y.-H. Li and M. Savvides, "An automatic iris occlusion estimation method based on high-dimensional density estimation," *Pattern Analysis and Machine Intelligence, IEEE Transactions on*, vol. 35, no. 4, pp. 784–796, April 2013.

[17] W. Sankowski, K. Grabowski, M. Zubert, and M. Napieralska, "Iris Finder–Program For Reliable Iris Localization In Images Taken Under Visible Light," *Journal of Medical Informatics & Technologies Selected full texts*, vol. 10, pp. 125–132, 2006.

[18] Y. Du, R. Ives, and D. Etter, "A new approach to iris pattern recognition," *Proceedings of SPIE*, pp. 1–12, 2004. [Online]. Available: http://citeseerx.ist.psu.edu/viewdoc/download?doi=10.1.1.107.4292\&rep=rep1\&type=pdf

[19] R. P. Wildes, "Iris recognition: an emerging biometric technology," *Proceedings of the IEEE*, vol. 85, no. 9, pp. 1348–1363, 1997. [Online]. Available: http://ieeexplore.ieee.org/lpdocs/epic03/wrapper.htm?arnumber=628669

[20] Y. Chen, S. C. Dass, and A. K. Jain, "Localized iris image quality using 2-D wavelets," *Advances in Biometrics*, pp. 0–6, 2005. [Online]. Available: http://www.springerlink.com/index/p34g247h453pn744.pdf

[21] Z. He, T. Tan, Z. Sun, and X. Qiu, "Toward Accurate and Fast Iris Segmentation for Iris Biometrics," *Pattern Analysis and Machine Intelligence, IEEE Transactions on*, vol. 31, no. 9, pp. 1670–1684, Sep. 2009. [Online]. Available: http://www.ncbi.nlm.nih.gov/pubmed/19574626

[22] R. Haralick, K. Shanmugam, and I. Dinstein, "Textural features for image classification," *Systems, Man and Cybernetics, IEEE Transactions on*, vol. 3, no. 6, pp. 610–621, 1973. [Online]. Available: http://ieeexplore.ieee.org/xpls/abs_all.jsp?arnumber=4309314

[23] D. Chetverikov, "Detecting defects in texture," in *International Conference on Pattern Recognition*, 1988, pp. 61–63.

[24] R. Meylani, A. Ertuzun, and A. Ercil, "A comparative study on the adaptive lattice filter structures in the context of texture defect detection," in *ICECS '96*, 1996, pp. Vol II: 976 – 979.

[25] A. Kumar, "Inspection of surface defects using optimal fir filters," in *ICASSP*, vol. II. IEEE, 2003, pp. 241–244.

[26] J. L. Sobral, "Optimised filters for texture defect detection," in *International Conference on Image Processing*, vol. III, 2005, pp. 565–568.

[27] H. Fujiwara, Z. Zhang, H. Toda, and H. Kawabata, "Textile surface inspection by using translation invariant wavelet transform," in *IEEE Int. Symp. on Computational Intelligence in Robotics and Automation*, vol. 3, IEEE. IEEE, 2003, pp. 1427 – 1432.

[28] H. Proena and L. A. Alexandre, "Introduction to the special issue on the segmentation of visible wavelength iris images captured at-a-distance and on-the-move," *Image and Vision Computing*, vol. 28, no. 2, pp. 213 – 214, 2010. [Online]. Available: http://www.sciencedirect.com/science/article/pii/S0262885609001905

[29] A. Telea, "An image inpainting technique based on the fast marching method," *Journal of graphics tools*, vol. 9, no. 1, pp. 23–34, 2004.

[30] J. Daugman, "High confidence visual recognition of persons by a test of statistical independence," *Pattern Analysis and Machine Intelligence, IEEE Transactions on*, vol. 15, no. 11, pp. 1148 –1161, Nov. 1993.

[31] M. Haindl, "Visual data recognition and modeling based on local markovian models," in *Mathematical Methods for Signal and Image Analysis and Representation*, ser. Computational Imaging and Vision, L. Florack, R. Duits, G. Jongbloed, M.-C. Lieshout, and L. Davies, Eds. Springer London, 2012, vol. 41, ch. 14, pp. 241–259, 10.1007/978-1-4471-2353-8_14. [Online]. Available: http://dx.doi.org/10.1007/978-1-4471-2353-8_14

[32] M. De Marsico, M. Nappi, and D. Riccio, "Noisy iris recognition integrated scheme," *Pattern Recognition Letters*, vol. 33, no. 8, pp. 1006–1011, 2012.

[33] H. Proença and L. A. Alexandre, "{UBIRIS}: A noisy iris image database," in *13th International Conference on Image Analysis and Processing - ICIAP 2005*, vol. LNCS 3617. Cagliari, Italy: Springer, 2005, pp. 970–977. [Online]. Available: http://www.springerlink.com/index/f707h158j67043v1.pdf

[34] H. Proença, S. Filipe, R. Santos, J. Oliveira, and L. Alexandre, "The ubiris.v2: A database of visible wavelength iris images captured on-the-move and at-a-distance," *Pattern Analysis and Machine Intelligence, IEEE Transactions on*, vol. 32, no. 8, pp. 1529 –1535, 2010.

[35] J. V. Kittler, R. Marik, M. Mirmehdi, M. Petrou, and J. Song, "Detection of defects in colour texture surfaces," in *IAPR Workshop on Machine Vision Applications*, 1994, pp. 558–567. [Online]. Available: ftp://ftp.ee.surrey.ac.uk/pub/vision/papers/mirmehdi-mva94.ps.Z

[36] P. Mitra, C. Murthy, and S. Pal, "Unsupervised feature selection using feature similarity," *IEEE Transactions on Pattern Analysis and Machine Intelligence*, vol. 24, no. 3, pp. 301–312, March 2002.

[37] M. Mirmehdi, R. Marik, M. Petrou, and J. V. Kittler, "Iterative morphology for fault detection in stochastic textures," *Electronic Letters*, vol. 32, pp. 443–444, 1996.